Oncology
and Radiotherapy ©
Vol.15 Iss.5:01-09 • Research Article

PET/MRI guided GTV delineation for radiotherapy planning in patients with locally advanced squamous cell carcinoma of the oropharynx and the oral cavity

N. Samołyk-Kogaczewska[1], E. Sierko[2], K. Zuzda[3], P. Gugnacki[3], K. Szczecina[4], D. Dziemianczyk-Pakieła[5], P. Szumowski[6], J. Burzynska-Sliwowska7, M. Mojsak[6]

[1] Department of Radiotherapy, NU-MED Diagnostics and Oncological Therapy Centre, Zamosc, Poland
[2] Department of Oncology, Medical University of Bialystok, Bialystok, Poland
[3] Student Scientific Society affiliated with the Department of Oncology, Medical University of Bialystok, Bialystok, Poland
[4] Department of Radiotherapy, Comprehensive Cancer Centre, Bialystok, Poland
[5] Department of Maxillofacial and Plastic Surgery, Medical University of Bialystok, Poland
[6] Laboratory of Molecular Imaging, Nuclear Medicine Department, Medical University of Bialystok, Bialystok, Poland
[7] Department of Diagnostic Imaging, Comprehensive Cancer Centre, Bialystok, Polandy

SUMMARY

Background: Evaluation of possibilities offered by PET/MRI in GTV definition of primary tumors during radiotherapy planning in patients (pts) with locally advanced carcinoma of the oral cavity and the oropharynx. Methods: 15 pts with SCC of the oral cavity and the oropharynx underwent CECT (Aquilion ONE, Toshiba) and PET/MRI (3T Siemens Biograph mMRI) examination. Delineation of GTV was done using two methods: visual interpretation of CT (GTV-CT), PET (GTV-PETvis) and MRI (GTV-MRI) images, as well as the quantitative automatic method (Syngovia, Siemens) based on a selected threshold value (20%, 30%, 40%, 50%) of SUVmax from a PET examination (GTV-PET20%, GTV-PET30%, etc). Obtained volumes were compared and differences were statistically analysed. Results: Statistical analysis demonstrated that GTV-MRI (p=0.0010), GTV-PET20% (p=0.0409), GTV-PET40% (p=0.0309) and GTV-PET50% (p=0.0018) diverged significantly from GTV-CT. The remaining measurements were not significantly different from GTV-CT. 73% of GTV-PETvis were inside the GTV-MRI contours. 27% of increased FDG uptake was present outside the GTV-MRI boundaries. Conclusions: Hybrid PET/MRI may provide improved accuracy in radiotherapy planning since it can identify regions of the tumor which are not clearly visible in other examinations. GTV-MRI, GTV-PET20%, GTV-PET40% and GTV-PET50% diverge significantly from GTV-CT.

Key words: PET/MRI, cancer, oral cavity, oropharynx, radiotherapy, GTV

Address for correspondence:

Ewa Sierko, Department of Oncology, Medical University of Bialystok, Ogrodowa 12, 15-027 Bialystok, Poland, e-mail: ewa.sierko@iq.pl ORCID ID: 0000-0001-6661-3182 N. Samołyk-Kogaczewska, Department of Radiotherapy, NU-MED Diagnostics and Oncological Therapy Centre, Zamosc, Poland, e-mail: natalia.samolyk@gmail.com ORCID ID: 0000-0002-9261-5728

Word count: 7134 **Tables:** 04 **Figures:** 04 **References:** 46

Received: - 19 April, 2021

Accepted: - 27 April, 2021

Published: - 19 May, 2021

INTRODUCTION

Head and Neck Cancers (HNC) are the sixth most common malignancies worldwide [1]. 60% of HNC patients present with non-metastatic, locally advanced disease (clinical stages III or IV) [2]. They require a multimodality approach and one of the main treatment methods in this group of patients is Radiotherapy (RT). Intensity Modulated Radiotherapy (IMRT) or Volumetric Arc Therapy (VMAT) is the most frequently employed RT techniques in such patients. These high precision techniques allow for conformal dose distribution and create very sharp dose gradients between radiation target volumes and organs at risk [3]. However, modern RT requires the use of various imaging modalities to adequately determine Gross Tumor Volume (GTV) [4,5]. The most widely used volumetric imaging methods such as Computed Tomography (CT) or Magnetic Resonance (MRI) rely on morphologically related parameters to distinguish between neoplastic and normal tissues. Functional imaging such as Positron Emission Tomography (PET) can facilitate this distinction, with visualization of foci with intensified 18F-Fluorodeoxyglucose (FDG) uptake, which is characteristic of areas of increased metabolism including carcinomas [6,7]. A recently introduced innovative fusion of PET and MRI combines the metabolic imaging capabilities of PET with the superb soft tissue contrast of MRI [7,8]. Studies on the usefulness and accuracy of PET/MRI in RT planning are currently in progress [4,8]. Initial results indicate that PET/MRI may contribute to treatment personalization and could provide increased accuracy than other methods of GTV determination in HNC patients [8,9]. It has been shown that PET/MRI improves the delineation of brain tumors in RT planning [10]. In the case of patients with advanced HNC, combining metabolic and anatomical information in the form of PET/MRI images, taken when the patient is in the same position, can facilitate precise determination of the target volume while reducing the risk of potential under- or over-treatment [2,11]. This is particularly important in HNC patients since the region contains organs at risk [11]. However, data regarding the usefulness of PET/MRI in RT planning in cancer of the oral cavity and the oropharynx are limited and inconsistent [8,9,12-14].

Precise definition of GTV is crucial and forms the basis for designing a personalised RT treatment plan. On the other hand, it is a time-consuming process which is prone to error [11,15]. A minor spatial error in target delineation can increase the risk of disease recurrence [16]. Data on PET-based delineation of GTV in HNC are limited and there are few published papers regarding the use of PET/MRI in HNC RT planning [8,9,12-14]. However, there are several PET-based delineating methods described in the literature such as visual tumor contouring, modalities based on Standardised Uptake Value (SUV), thresholding, source/background algorithms, and other automatic or semi-automatic methods [12,17,18]. Visual (manual) and quantitative threshold-based methods were employed in our study since these are the most commonly used modalities.

The purpose of the study was to assess the possibilities offered by innovative hybrid PET/MRI in the GTV definition of primary tumors in RT planning in patients with locally advanced carcinoma of the oral cavity and the oropharynx.

MATERIALS AND METHODS

A group of 15 patients (nine female and six male) with locally advanced squamous cell carcinoma of the oral cavity and oropharynx were included in the prospective study between July 2016 and February 2018. Inclusion criteria were as follows: age over 18 years old, absence of uncontrolled systemic diseases, no history of prior hypersensitivity or allergic reaction to an intravenous contrast or FDG, glycaemic blood level under 160 mg/dl, absence of metal devices in the body (cardiac pacemakers, cochlear implants, intrauterine contraceptive devices, metal shavings in the eyeball, surgical clips, metal surgical stitches). All subjects provided informed consent for study participation and PET/MRI. Written information regarding the study was given to each participant.

Based on CT evaluation, patients were found to be in clinical stages III or IV of the disease. The floor of the mouth was the primary tumor location in four patients, base of the tongue in four patients, oral tongue in three patients, buccal mucosa in two patients, lower gingiva in one patient and the submandibular salivary gland in one patient. Characteristics of study participants are presented in Table 1.

The group was homogeneous in terms of a full blood count and electrolyte blood count test results, thyroid hormone levels as well as renal and liver function parameters. Four patients had increased C Reactive Protein (CRP) concentration, with values between 9.1 mg/l and 51.1 mg/l (the upper limit of the normal range is 5 mg/l). Those patients had no symptoms of systemic or local infection.

Patients underwent a routine, contrast-enhanced, 3 mm slice thickness CT scan (Ultravist 300, 1 ml/kg) of the head and neck region on a 320-slice CT scanner (Aquilion ONE, Canon Medical Systems Corporation, Otawara, Japan). PET/MRI examinations were conducted within an average of 14 days (range of 6-23 days) of the CT scan on 3 Tesla Siemens Biograph mMR scanner (Siemens Healthcare GmbH, Erlangen, Germany). Sixty minutes prior to image acquisition the subjects received approximately 4 MBq/kg (range of 203 MBq-417 MBq) of intravenous 18F-FDG. The first stage of the examination was whole-body, low resolution MRI imaging, followed by static PET scanning and diagnostic MRI scanning (T1- and T2-weighted sequences and contrast-enhanced sequences, Gadovist 1.0, 0.1 ml/kg, with 3D distortion correction) of the head and neck region. MRI attenuation images were acquired using the Dixon approach with a coronal 2-point 3D T1-weighted Volumetric Interpolated Breath Hold Examination (VIBE) [3.12 mm slice thickness, 20% interslice gap, integrated parallel acquisition technique factor 2, acquisition time 19s, 192 × 121 matrix, 500 mm × 328 mm Field of View (FOV), repetition time 3.6 ms, echo time 1.23 ms and 2.46 ms]. PET/MRI scans were obtained simultaneously in the same patient position. No immobilisation specific for RT (head and neck Orfit mask) was used during the PET/MRI examination.

Contours of the primary tumors were defined by a highly experienced radiation oncologist in cooperation with a radiologist and a nuclear medicine specialist. GTVs were delineated using two different methods. The first was visual interpretation of CT

Tab. 1. Characterisation of locally advanced oral cavity and oropharynx SCC patients according to HP, histology grade score, proliferation index Ki67 expression, TNM clinical stage classification (AJCC, ed. 8, 2017), based on Computed Tomography (CT) evaluation, status of p16 protein, Human Papilloma Virus (HPV) infection, Epstein-Barr Virus (EBV) infection, smoking status and biopsy performed before Positron Emitted Tomography/Magnetic Resonance imaging (PET/MRI)

No. of pts	H-P	G	Ki67	TNM	p16 status	HPV status	EBV status	smoking	Biopsy before PET/MR (days)
1	SCC	2	30%	T3N0M0	1	1	0	Yes	Yes (34)
2	SCC	2	N/A	T3N2cM0	N/A	N/A	N/A	Yes	Yes (25)
3	SCC	2	N/A	T3N2cM0	N/A	N/A	N/A	No	Yes (18)
4	SCC	2	20%	T4N0M0	0	0	0	Yes	Yes (20)
5	SCC	2	20%	T3N1M0	0	0	0	Yes	Yes (21)
6	SCC	1	20%	T4N2bM0	0	0	0	Yes	Yes (20)
7	SCC	2	30%	T3N2bM0	0	0	1	Yes	Yes (28)
8	SCC	2	30%	T3N1M0	0	0	0	No	Yes (20)
9	SCC	2	60%	T3N1M0	1	0	0	No	Yes (25)
10	SCC	2	N/A	T3N0M0	N/A	N/A	N/A	Yes	Yes (21)
11	SCC	2	30%	T4N3M0	0	0	0	Yes	Yes (15)
12	SCC	2	N/A	T3N2cM0	N/A	N/A	N/A	Yes	Yes (21)
13	SCC	1	N/A	T4N2bM0	N/A	N/A	N/A	Yes	Yes (32)
14	SCC	2	30%	T3N0M0	0	0	0	No	Yes (15)
15	SCC	3	20%	T3N1M0	0	0	0	No	Yes (20)

H-P: Histopathology; G: histology grade score; SCC: Squamous Cell Carcinoma; 1: positive; 0: negative; N/A: Not Available

(GTV-CT), MRI (GTV-MRI) and PET (GTV-PETvis) images. GTV-CT was delineated on axial slices of contrast-enhanced CT scans and GTV-MRI on a T1-weighted VIBE Dixon MRI sequence. Both, GTV-CT and GTV-MRI were defined on the Oncentra system (Nucletron, Veenendaal, Netherlands). The GTV-CT was created without knowledge of the PET/MRI images. Target volumes on PET images were manually created using the Wacom Intuos Draw graphics tablet (Wacom Co Ltd., Saitama, Japan) on a PET-workstation with syngo. *via* VB10B software (Siemens Healthcare GmbH, Erlangen, Germany). GTV-PETvis were obtained using the 'halo' method described by Ashamalla et al. [19]. The 'halo' area was recognisable by its specific colour, a slim wall and a low SUV area located around the region of the maximal metabolic activity of the tumor [19]. GTV-PETvis was defined on the spectrum window level in syngo. *via* software.

The quantitative automatic method based on a selected threshold value: 20%, 30%, 40%, 50% of SUVmax (maximal SUV) from the PET examination was the second GTV delineation method. The received volumes were named: GTV-PET20%, GTV-PET30%, GTV-PET40%, GTV-PET50%, respectively. Tumor volumes were obtained using an automatic contour function-the Volume of Interest Isocontour (VOI) in syngo.*via* software on a PET-workstation. A 'sphere' was placed over the area of high FDG uptake and the contour was obtained automatically by applying selected values of SUVmax thresholds (Figure 1).

Statistical analysis of differences in GTV values obtained from CT, PET and MRI was performed. GTV-CT was used as the reference examination since the majority of currently used radiotherapy planning systems is based on contrast-enhanced CT. Moreover, the majority of guidelines for delineating GTV and organs at risk in the head and neck region published by reputable radiation oncologist associations are based on the evaluation of CT images [20-22]. The evaluation of the normality of the distribution was carried out with the Shapiro-Wilk test. The data were paired Wilcoxon test. The level of significance was $p<0.05$.

Spatial analysis between GTV-MRI, GTV-PETvis and GTV-CT was performed using the Dice Similarity Coefficient (DSC) and the modified Hausdorff Distance (mHD). Moreover, DSC and mHD between tumor volumes on CT (GTV-CT) and hybrid PET/MRI (GTV-PET/MRI) were also measured. Images from CT, MRI and PET scans were fused using rigid registration in Oncentra (Nucletron, Veenendaal, Netherlands) with a mutual information algorithm (shifts and rotation relative to the shape and volume of anatomical structures). Registration accuracy between CT and PET/MRI images was reported qualitatively. GTV-PETvis were redefined in Oncentra by the same radiation oncologist as before, also using the 'halo' method, based on previously specified contours on PET images. GTV-PET/MRI was created as a fusion of GTV-MRI and GTV-PETvis volumes on PET/MRI images. DSC was calculated using the equation: $2 \times (A \cap B)/(A+B)$, where A and B represent two volumes, $(A \cap$

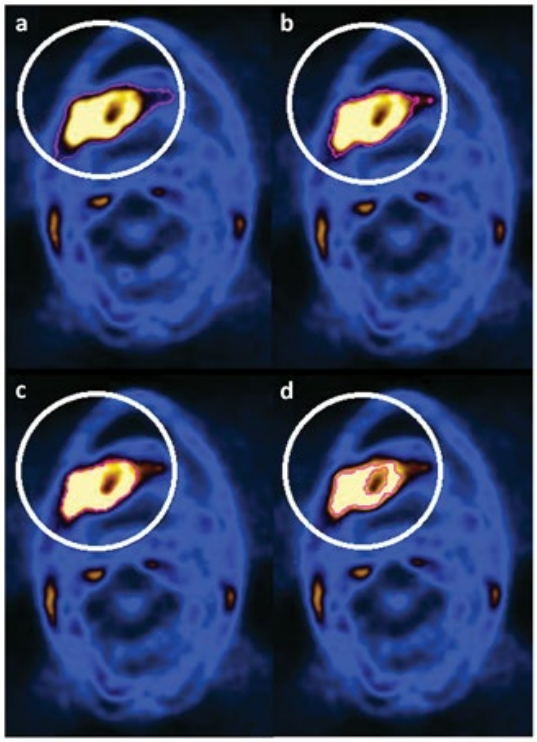

Fig. 1. Comparison of primary tumor (GTV, Gross Tumor Volume) delineation using automatic fixed threshold method in a patient with squamous cell carcinoma of the floor of the mouth (T4N0M0); (a) GTV obtained with a threshold of 20% of SUV_{max} (maximum standardized uptake value); (b) threshold of 30% of SUV_{max}; (c) threshold of 40% of SUV_{max}; (d) threshold of 50% of SUV_{max}

Tab. 2. The assessments of maximal and mean Standardized Uptake Value (SUV) of primary tumor and mean SUV of soft tissue obtained from 18-Fluorine-labeled Fluorodeoxyglucose Positron Emitted Tomography (18F-FDG-PET) images in patient (1-15) with locally advanced squamous cell carcinoma of the oral cavity and oropharynx

No. of pts	1	2	3	4	5	6	7	8	9	10	11	12	13	14	15
Tumor SUV_{max}	8,05	9,71	13,7	10	9,25	12,1	11,5	11.9	17,8	20,6	12,3	22,3	8,82	14,8	17
Tumor SUV_{mean}	5,1	5,63	8,73	5,56	5,56	7,09	7,37	7,68	10,7	12,4	7,26	14,2	4,87	8,9	10,1
Soft tissue SUV_{mean}	0,5	0,6	0,52	1,09	0,42	0,63	0,43	0,47	0,61	0,67	0,44	0,55	0,51	0,49	0,48
Tumor SUV_{max}/soft tissue index	16,1	16,18	26,35	9,17	22,02	19,21	26,74	25,31	29,18	30,75	27,95	50,68	17,3	30,2	35,4
Tumor SUV_{mean}/soft tissue index	10,2	9,38	16,79	5,1	13,2	11,25	17,14	16,34	17,54	18,51	16,5	25,8	9,54	18,16	21

SUV_{max}: maximal standardized uptake value; SUV_{mean}: mean standardised uptake value

B) represents the volume of intersection, and (A+B) represents the absolute sum of their volumes [14]. DSC values are between 0 and 1, where DCS of 0 indicates no spatial overlap at all and a DSC of 1 indicates a complete overlap. The mHD measures similarity between two volumes by reporting the mean orthogonal distance between surface points [23].

RESULTS

Measurements of primary tumor SUV_{max}, SUV_{mean} and correction of SUV values for healthy soft tissue are presented in Table 2.

In 87% of GTV-MRI (mean GTV 40.5 cm^3) and 80% of GTV-PETvis (mean GTV 31.7 cm^3) volumes were larger than the reference GTV-CT (mean GTV 26.1 cm^3). The mean difference between GTV-MRI and GTV-CT was 16.6 cm^3 (range 1.9 cm^3-40.3 cm^3). On the other hand, the mean difference between GTV-PETvis and GTV-CT was 10.3 cm^3 (range 1.9-18.4 cm^3). GTV-MRI and GTV-PETvis were similar to GTV-CT in two and three cases, respectively. 32% of all PET-based threshold measurements (mainly GTV-PET20% and GTV-PET30%) were larger than the results based on CT images. The mean difference between GTV-CT and GTV-PET20% was 21.3 cm^3 (range 1.6-71.4 cm^3), GTV-PET30%-11.6 cm^3 (range 2-34.8 cm^3). In two cases GTV-PET40% was larger than GTV-CT-the difference was 16.3 cm^3 and 9.8 cm^3. In the same two patients, GTV-PET50% was larger than GTV-CT-the differences were 4.6 cm^3 and 4.9 cm^3. On the other hand, 63% of volumes from the quantitative automatic method (mostly GTV-PET40% and GTV-PET50%) were smaller than GTV-CT. GTV-PET40% and GTV-PET50% were, respectively, approximately 13.1 cm^3 (range 2.1 cm^3-44.8 cm^3) and 17.9 cm^3 (range 2.9 cm^3-53.5 cm^3), smaller than GTV-CT. The mean difference between GTV-CT and GTV-PET20% was 10.1 cm^3 (range 2.1 cm^3-22.6 cm^3), GTV-PET30% -12.7 cm^3 (2.8 cm^3-34.6 cm^3). In three cases, GTV values obtained using the threshold-based method was close to GTV-CT. Obtained GTV measurements are presented in Table 3.

Statistical analysis (Figure 2) revealed that primary tumor volumes obtained from GTV-MRI (p=0.0010), GTV-PET20% (mean GTV volume 37.7 cm^3, p=0.0409), GTV-PET40% (mean GTV volume 16.8 cm^3, p=0.0309) and GTV-PET50% (mean GTV volume 11.7 cm^3, p=0.0018) diverged significantly from the volumes based on CT images. Conversely, GTV-PETvis (p=0.0691) and GTV-PET30% (mean GTV volume 23.6 cm^3, p=0.8927) were not significantly different compared to the reference GTV-CT.

Volumes obtained from PET images using the visual-based delineation method were inside the GTV-MRI contours in around 73% of cases. In 27% of cases, increased FDG uptake was present outside the GTV-MRI boundaries (Figure 3).

In the subgroup of patients with increased CRP concentration, GTV-PETvis was larger than GTV-CT in one case and smaller in two cases. In one case, GTV-PETvis volume was similar to the obtained GTV-CT. Due to a small number of subjects in this subgroup, statistical analysis was not performed. Moreover, artefacts from dental restorations, which obscured oral cavity structures and impeded target volume delineation on CT scans, were observed in seven patients (47%) (Figure 4).

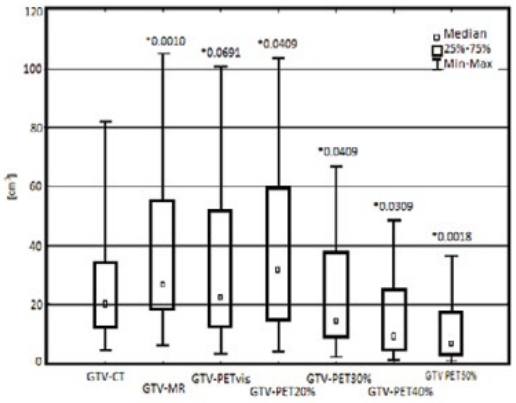

Fig. 2. Statistical comparison of primary tumor volumes (Gross Tumor Volume, GTV) delineated using the visual method and fixed threshold method, obtained from Computed Tomography (CT), Magnetic Resonance Imaging (MRI) and 18-fluor-labelled fluorodeoxyglucose Positron Emitted Tomography (PET) images. The graph shows the median, the average, and the level of statistical significance p (*) of obtained results

Tab. 3. Results of the volumetric assessments of primary tumor volumes (Gross Tumor Volume, GTV) obtained from Computed Tomography (CT), Magnetic Resonance Imaging (MRI) and 18-Fluorine-labeled Fuorodeoxyglucose Positron Emitted Tomography (18F-FDG-PET) images in patients with locally advanced carcinoma of the oral cavity and the oropharynx

pts	GTV-CT (cm^3)	GTV-MR (cm^3)	GTV-PETvis (cm^3)	GTV-PET20% (cm^3)	GTV-PET30% (cm^3)	GTV-PET40% (cm^3)	GTV-PET50% (cm^3)
1	32,12	60	59,32	103,53	66,9	48,45	36,72
2	12,16	11,4	12,32	27,74	9,33	4,65	2,84
3	82,23	93,59	100,6	94,07	60,42	47,09	35,59
4	35,65	55,02	51,81	59,11	37,6	28,3	18,56
5	13,97	22,57	16,08	39,49	13,62	8,14	4,97
6	4,35	6,23	3,26	7,77	3,48	2,24	1,42
7	21,34	48,6	23,24	31,74	23,36	17,68	13,03
8	11,24	18,11	7,75	12,87	7	3,99	1,76
9	5,89	16,17	6,73	3,77	2,17	1,31	0,86
10	20,23	23,88	15,02	15,02	14,49	9,26	6,59
11	26,24	26,84	18,56	15,92	10,64	7,17	4,32
12	12,33	41,1	24,08	36,41	27,82	22,14	17,23
13	34,18	55,37	36,35	60,08	38,21	25,27	15,73
14	64,8	105,12	77,67	42,24	30,2	19,97	11,26
15	15,06	23,97	22,43	15,46	8,73	5,97	4,12

PETvis: visual method; PET20%, PET30%, PET40%, PET50%: volumes covered by 20%, 30%, 40%, 50% threshold of maximal Standardized Uptake Value (SUV_{max}), respectively

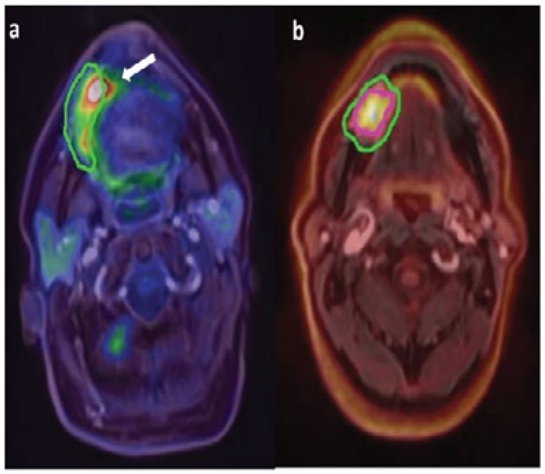

Fig. 3. Primary tumor volume (GTV, Gross Tumor Volume) delineated with the manual method and presented on a fusion of 18-fluor-labelled fluorodeoxyglucose Positron Emitted Tomography (PET) and Magnetic Resonance Imaging (MRI) images; (a): PET-based GTV (arrow) is partly outside MRI-based GTV (green line) in the case of a patient with squamous cell carcinoma of the right lower gingiva (T4N2bM0), GTV-PET defined on spectrum window level; (b): PET-based GTV (pink line) is included in larger MRI-based GTV (green line) in the case of a patient with squamous cell carcinoma of the floor of the mouth (T3N1M0), GTV-PET defined on the hot iron window level

In these cases, MRI showed the primary tumor area more precisely than CT scanning. In five patients from this subgroup, GTV-PETvis volumes were more closely related to GTV-CT than to GTV-MRI. All of the MRI-based primary tumor volumes in patients with artefacts from metallic dental work were larger than GTV-CT. Volumes of GTV-PETvis were smaller than those of GTV-CT in four patients, and larger than reference volumes in the remaining cases. There was not a single SUV_{max} threshold value whose application could create volumes similar to GTV-CT in this subgroup of patients. All of the GTV-PETvis volumes and 87.5% (seven patients) of GTV-MRI volumes were larger than GTV-CT volumes in patients without dental restorations (eight patients). DSC and mHD for GTV-MRI, GTV-PETvis, GTV-PET/MRI and GTV-CT are presented in Table 4.

The average value of DSC for GTV-CT and GTV-MRI was 0.74 (range 0.54-0.88) and for GTV-CT and GTV-PETvis-0.78 (range 0.67-0.9). The average mHD between GTV-CT and GTV-MRI was 17.4 mm (range 4 mm-29 mm), and between GTV-CT and GTV-PETvis- 16.9 mm (range 5 mm-28mm). The values of mHD and DSC for GTV-CT and GTV PET/MRI were in the range of 0 mm-24 mm (Average 13.3 mm) and

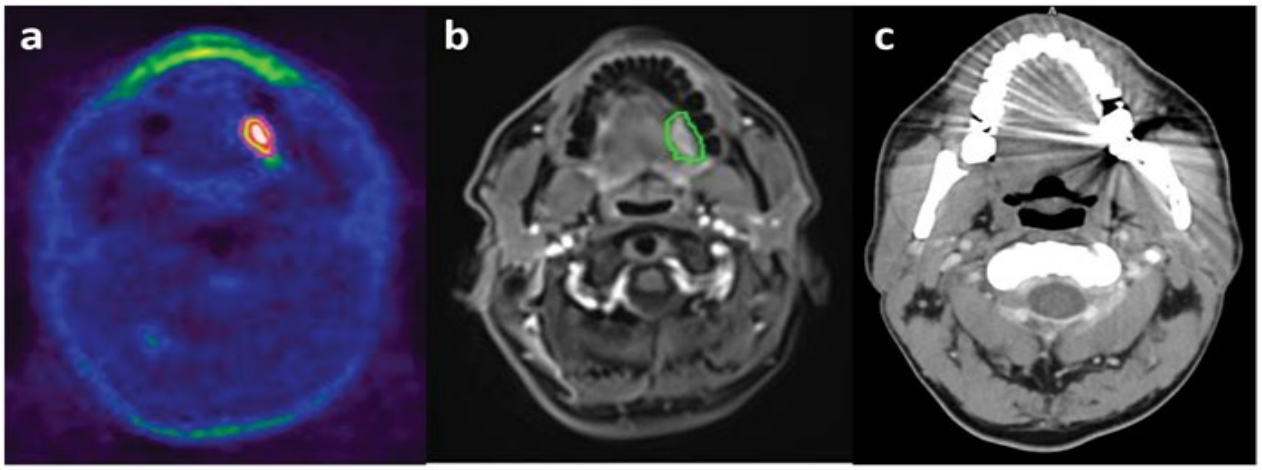

Fig. 4. Patient with squamous cell carcinoma of the base of the tongue (T3N0M0) and dental restoration in the left second molar tooth. Primary tumor volume delineated with the manual method and presented on: (a) 18-Fluor-labelled Fluorodeoxyglucose Positron Emitted Tomography (PET) image (pink line), (b) Magnetic Resonance (MRI) image (green line), (c) primary tumor volume is invisible on the Computed Tomography (CT) image due to extensive artefacts from dental restoration

Tab. 4. Spatial correlation between Gross Tumor Volume (GTV) obtained from Computed Tomography (GTV-CT), Magnetic Resonance (GTV-MRI), Positron Emitted Tomography (GTV-PETvis) and hybrid of Positron Emitted Tomography/ Magnetic Resonance (GTV-PET/MRI) in patients with locally advanced squamous cell carcinoma of the oral cavity and oropharynx (1-15)

No. of pts	1	2	3	4	5	6	7	8	9	10	11	12	13	14	15	Average
mHD [mm] between:																
GTV-CT and GTV-MRI	19	18	17	24	11	4	29	11	26	18	14	21	18	14	17	17,4
GTV-CT and GTV-PET_{vis}	19	21	20	23	11	5	24	12	18	8	15	28	17	13	19	16,9
GTV-CT and GTV-PET/MRI	20,3	20,6	0	21	11	4,1	24	12	19	0	0	20	18	14	15	13,3
DCS for:																
GTV-CT and GTV-MRI	0,68	0,71	0,8	0,54	0,79	0,77	0,88	0,68	0,7	0,85	0,74	0,7	0,78	0,82	0,7	0,74
GTV-CT and GTV-PET_{vis}	0,78	0,79	0,79	0,76	0,67	0,72	0,82	0,8	0,79	0,73	0,7	0,76	0,77	0,9	0,72	0,78
GTV-CT and GTV-PET/MRI	0,64	0,82	0	0,71	0,75	0,77	0,81	0,75	0,79	0	0	0,82	0,77	0,84	0,74	0,61

Pts: patients; PET_{vis}: visual method of GTV delineation; DSC: Dice Similarity Coefficient; mHD: modified Hausdorff distance

0 mm-0.84 mm (average 0.61 mm), respectively. Registration accuracy between CT and PET/MRI was high, almost perfect in 4/15 cases, not very good or poor in remaining cases.

DISCUSSION

The visual method is based on hand-drawn boundaries of the region of interest. It is a subjective interpretation of images, so it could lead to inter- and intra-observer errors. To minimise inter-observer variation delineation should be made by a single, well-trained observer or automatic systems [5,16]. In a study by Ashamalla et al. [19], the 'halo' method, utilised in our study for GTV-PETvis contouring, resulted in a reduction in inter-observer variability as well as modification of GTV in 53% of cases when compared with GTV-CT. Moreover, in the case of PET imaging, settings of the window levels resulted in significantly different tumor volumes [16,18,24]. Visual delineation requires the use of standardised protocols of image reconstruction and display setting to improve conformity [18].

In the present study, primary tumour volumes obtained using the visual method based on MRI and PET images were larger in 87% and 80% of cases, respectively, when compared to the reference GTV-CT. However, differences between GTV-CT and GTV-PETvis were not statistically significant. Other authors have obtained similar results [25]. In our other study [26], we revealed that 80% of GTV-MRI and 40% of GTV-PETvis were larger than GTV-CT. Bruela et al. [16] reported that in 55% of cases PET-based GTV were larger than GTV-CT, but the differences were not statistically significant. The higher percentage of cases with GTV-PETvis larger than GTV-CT may be related to false positive findings due to peritumoral inflammation [27]. Squamous cell HNC is highly inflammatory in nature, particularly in advanced stages [28]. The probable peritumoral inflammation associated with large tumors investigated in the present study might have led to increased target volume during GTV-PETvis delineation. However, among patients with increased CRP concentration in our study, in only one out of four cases was GTV-PETvis larger than GTV-CT.

Other authors have observed a significant decrease in tumor volume in MRI-based delineation in comparison to GTV-CT [13]. Wang et al. [14] revealed that volumes obtained from manual delineation based on PET/MRI and CT images were similar in size. The same authors reported individual cases with larger volumetric differences due to improved visualisation of the primary tumour on PET/MRI, but the findings were not statistically significant. Contrary to our results, other studies have demonstrated that GTV-CT was significantly larger when compared to GTV-PET [11,24]. Daisine et al. [29] did not reveal any significant differences between GTVs based on CT and MRI images, but average GTV-PET were smaller than both GTV-CT and GTV-MRI. Significant differences between GTV-CT and GTV-MRI in the present study may also have resulted from the presence of dental restoration artefacts in 47% of cases, which substantially decreased the visibility of the tumor on CT scans and improved tumors visualisation on MRI scans due to improved soft tissue imaging [8,30]. In our study, all GTV-MRI volumes were larger than GTV-CT in the subgroup of patients with dental artefacts. On the other hand, metallic dental restorations such as dental crowns and amalgam fillings can also interfere with magnetic field-induced image artefacts [31]. Even small amounts of a ferromagnetic substance can cause an extensive blank in a MRI image [32]. The magnitude of the effect correlates with the actual size of the artefact, but PET/MRI image artefacts may exceed the real volume of dental restorations [33]. However, artefacts on MRI scans rarely impair anatomical assessment of the examined region and do not cause a deformation, obstruction or excision of parts of the image, as is the case with CT scanning [32]. In the case of PET scans, Ladefoget et al. [33] reported that bias in attenuation correction related to dental artefacts can be observed. The bias depends on the size and location of the artefact. In consequence, imaging of FDG uptake in the area where the tumour is obscured by an artefact can be considerably reduced [33]. This could explain our results obtained in the subgroup of patients with artefacts, where GTV-PETvis were smaller in four out of seven cases compared to GTV-CT. Conversely, in the subgroup of patients without artefacts, all of the eight GTV-PETvis cases were larger than GTV-CT.

The fixed threshold method is the second most frequently utilised modality in target volume delineation. There is still no consensus regarding the universal SUV threshold value for target volume delineation. However, threshold values of 40% and 50% of SUV_{max} are predominantly applied and described in the literature [8,13,18,27,34-41]. Ferrando et al. [27] used the adaptive threshold method in 30 patients and demonstrated that threshold values in the range of 20%-41% were those most suited for primary tumor volume definition. However, other authors using thresholds in the range of 10%-50% have not been able to select an ideal value for GTV delineation [34]. In the present study, GTV based on the threshold of 30% of SUV_{max} was statistically the most closely related to GTV-CT. Out of all the SUV_{max} threshold-based method measurements, 32% of PET GTVs were larger, whereas 63% were smaller than GTV-CT. Paulino et al. [35] reported that 75% of GTV-PET50% were smaller than GTV-CT. In a study by Chauhan et al. [13], 60% of GTV-PET40% was larger than GTV-CT. The authors believed that the obtained results were secondary to the presence of oedema, inflammation or PET avid areas, such as tonsils, mastication muscles and salivary glands in the immediate vicinity of target volumes. In our previous study [26], statistical analysis confirmed that in 50% of patients GTV-PET30% were the most closely related volumes to GTV-CT out of all threshold methods. Other authors have demonstrated that 62% of PET-based GTV cases were larger than GTV-CT and 38% were smaller, respectively [33]. The authors indicated 36%-44% of SUV_{max} as the optimal threshold value for the definition of the primary tumor volume larger than 4 ml. Difficulty in determining one universal threshold value may be associated with tumor heterogeneity and a lack of uniformity in FDG uptake, particularly in advanced tumors, which is related to the presence of hypoxia or necrosis in large tumors [34]. Tumour cell hypoxia is present in the majority of squamous cell HNC [42]. However, FDG has limited application in hypoxia imaging [42,43]. The use

of 18F-Fluoromisonidazole (FMISO) and 18F-Fluoroazomycin Arabinoside (FAZA) is recommended in clinical practice in such situations, but their availability is problematic in most radiation therapy centres [43,44]. Moreover, GTV delineation with the fixed threshold method has been tested on phantoms with symmetrical volumes, homogeneous activity and sharp borders [13]. Some authors have indicated that this contouring method has limited application, since tumors have complex shapes and blurred borders [13, 38].

Mismatch analysis is a potential tool for evaluating disparity between GTV obtained from anatomical and metabolic imaging. In our study, discrepancies between MRI- and PET-based tumor volumes were observed in 27% of patients. The differences regarded volumes which were visualised on PET, but were poorly visualised or invisible on MRI scans. Some authors have suggested that PET may identify tumor volume which is not clearly visible on anatomical imaging scans and could prevent spatial errors, particularly in regard to oral cavity lesions [16,27]. Ma et al. [8] reported that the total overlap of GTV-MRI and GTV-PET was approximately 90%. On the other hand, false-positive and false-negative overlap at the level of 10% indicates that further metabolic information and a larger sample size are needed. Other authors have demonstrated marginal or statistically insignificant discrepancies between PET and MRI. Kao et al. [34] concluded that mismatches might be related to the low spatial resolution of PET, with limitation of voxel density or partial volume effect.

Spatial analysis of GTV obtained by using different imaging methods was conducted using DSC and mHD. DSC has a limited range (0-1), where 0 indicates no spatial overlap and DSC of 1 indicates perfect overlap. The higher the DICE index (i.e.> 0.5), the higher the agreement [37]. Some investigators have reported that DSC 0.7 is a 'good' overlap and that DSC may vary more considerably with changes in size and less markedly with shape of the compared volumes [45]. Our results show that spatial compliance between GTV-CT/GTV-MRI and GTV-CT/GTV-PETvis is high with mean DSC values above 0.7 (0.74 and 0.78, respectively) for both compared GTV pairs. The modified Hausdorff distance is best for matching two objects based on their edge points [23]. A smaller mHD value, measured in millimetres, suggests that similarity between the compared volumes is greater [14]. Based on mean mHD values in our study, similarity between GTV-CT/GTV-MRI and GTV-CT/GTV-PETvis is suboptimal. The reason for this may be that mHD is a parameter which is more sensitive to changes in the shape of measured contours.

Spatial analyses of GTV-CT and GTV-PET/MRI volumes revealed reasonably good, but not perfect overlap (mean DSC 0.61 mm and mHD 13.3 mm). This could be related to different positioning due to a lack of patient immobilisation during imaging tests and the time interval between CT and PET/MRI examinations. If both tests had been conducted on immobilised patients immediately after each other, the observed changes in patient positioning would have been minimised. Mean mHD might have been affected by rather poor registration accuracy between CT and PET/MRI images. Since mHD depends on relative locations of end points of two contours, low accuracy of two images overlay may cause in increase in the distance between GTV-CT and GTV-PET/MRI end points. Similarly, in the case of DSC as a ratio of two areas overlay, not very good registration accuracy has an impact on the convergence of GTV-CT and GTV-PET/MRI.

One has to bear in mind when using PET in RT planning that SUV_{max} is a value of the point [8]. There are various factors that can influence SUV_{max} such as the patient's blood glucose level, the time between FDG injection and image acquisition, scan duration or technical aspects of the procedure (i.e. reconstruction parameters) [24]. Additionally, small, superficial, mucinous, well-differentiated or Human Papilloma Viruses-related (HPV-related) tumors can demonstrate low-grade or no 18FDG uptake [46].

The subject of this study requires further research on a larger cohort. Imaging tests should be performed with the use of patient immobilisation equipment. Comparison of PET/MRI and PET/CT accuracy in primary tumor delineation would have a great clinical value. Histopathological verification of PET/MRI-based GTV will be a valuable element in prospective trials. It would allow for the verification of PET/MRI accuracy in target volume imaging, determine true biological tumor volume and may indicate the most appropriate GTV delineating method.

In summary, there is no universal concept in terms of the best GTV delineation method in HNC patients. However, beside its limitations, PET/MRI has a technical advantage in metabolic and anatomical co-registration in tumor detection and target definition. Functional imaging may provide biological information allowing for 'dose painting' or dose escalation to tumor sub-volumes [4,18]. GTV-PETvis and GTV-PET30% seem to be good GTV delineation methods and further research could verify the usefulness of these two methods by evaluating correlations with endpoints such as local control, disease free survival.

CONCLUSIONS

Hybrid PET/MRI is useful in GTV delineation in patients with oral cavity and oropharyngeal cancers. This innovative imaging technique may improve accuracy of RT planning since it can identify parts of the tumor which are not clearly visible in other examination. Besides, GTV-MRI, GTV-PET20%, GTV-PET40% and GTV-PET50% diverge significantly from GTV-CT. Conversely, GTV-PETvis and GTV-PET30% were not significantly different compared to GTV-CT. However, further studies on larger groups of patients are needed.

PATENTS

Funding

The study was supported by a grant from the Leading National Research Centre (KNOW, Krajowy Naukowy Ośrodek Wiodący), Medical University of Bialystok, under award number KNOW-0600-SD63-1/2016.

Acknowledgment

The authors would like to express their thanks to Dorota Jurgilewicz. M.D. and Marcin Hladunski for their fruitful expert and technical assistance during study realization.

CONFLICTS OF INTEREST

The authors declare no conflict of interest.

REFERENCES

1. Vigneswaran N, Williams MD. 2014. Epidemiologic trends in head and neck cancer and aids in diagnosis. Oral Maxil Surg Clin. 2014;26:123-141.
2. Farina E, Ferioli M, Castellucci P, Farina A, Rambaldi G, et al. 2017. 18F-FDG-PET-guided planning and re-planning (adaptive) radiotherapy in head and neck cancer: current state of art. Anticancer Res. 2017;37:6523-6532.
3. Differding S, Hanin FX, Grégoire V. PET imaging biomarkers in head and neck cancer. Eur J Nucl Med Mol Imaging. 2015;42:613-622.
4. Roberts P, Jani A, Packianathan S, Albert A, Bhandari R, et al. Upcoming imaging concepts and their impact on treatment planning and treatment response in radiation oncology. Radiat Oncol. 2018;13:146.
5. Rutkowski T. The role of tumor volume in radiotherapy of patients with head and neck cancer. Radiat Oncol. 2014;9:23.
6. Verma V, Choi JI, Sawant A, Gullapalli RP, Chen W, et al. Use of PET and other functional imaging to guide target delineation in radiation oncology. Semin Radiat Oncol. 2018;28:171-177.
7. Niklinski J, Kretowski A, Moniuszko M, Reszec J, Michalska-Falkowska A, et al. Systematic biobanking, novel imaging techniques, and advanced molecular analysis for precise tumor diagnosis and therapy: The Polish MOBIT project. Adv Med Sci. 2017;62: 405-413.
8. Ma JT, Han CB, Zheng JH, Sun HZ, Zhang SM, et al. Hybrid PET/MRI-based delineation of gross tumor volume in head and neck cancer and tumor parameter analysis. Nucl Med Commun. 2017;38:642-649.
9. Winter R, Leibfarth S, Schmidt H, Zwirner K, Mönnich D, et al. Assessment of image quality of a radiotherapy-specific hardware solution for PET/MRI in head and neck cancer patients. Radiother Oncol. 2018:128:485-491.
10. Platzek I, Beuthien-Baumann B, Schneider M, Gudziol V, Langner J, et al. PET/MRI in head and neck cancer: initial experience. Eur J Nucl Med Mol Imaging. 2013;40:6-11.
11. Leclerc M, Lartigau E, Lacornerie T, Daisne J, Kramar A, et al. Primary tumor delineation based on 18FDG PET for locally advanced head and neck cancer treated by chemo-radiotherapy. Radiother Oncol. 2015;116:87-93.
12. Grégoire V, Thorwarth D, Lee J. Molecular imaging-guided radiotherapy for the treatment of head-and-neck squamous cell carcinoma: Does it fulfill the promises? Semin Radiat Oncol. 2018;28:35-45.
13. Chauhan D, Rawat S, Sharma M, Ahlawat P, Pal M, et al. Improving the accuracy of target volume delineation by combined use of computed tomography, magnetic resonance imaging and positron emission tomography in head and neck carcinomas. J Can Res Ther. 2015;11:746-751.
14. Wang K, Mullins BT, Falchook AD, Lian J, Huang B, et al. Evaluation of PET/MRI for tumor volume delineation for head and neck cancer. Front Oncol. 2017;7:8.
15. Schakel T, Peltenburg B, Dankbaar JW, Cardenas C, Aristophanous M, et al. Evaluation of diffusion weighted imaging for tumor delineation in head-and-neck radiotherapy by comparison with automatically segmented 18 F-fluorodeoxyglucose positron emission tomography. Phys Imaging Radiat Oncol. 2018;5:13-18.
16. Burela N, Soni T, Patni N, Bhagat J, Kumar T, et al. A quantitative comparison of gross tumor volumes delineated on [18F]-FDG-PET/CT scan and contrast-enhanced computed tomography scan in locally advanced head and neck carcinoma treated with Intensity Modulated Radiotherapy. Adv Mod Oncol Res. 2017;3:143-151.
17. MacManus M, Nestle U, Rosenzweig KE, Carrio I, Messa C, et al. Use of PET and PET/CT for radiation therapy planning: IAEA expert report 2006-2007. Radiother Oncol. 2009;91:85-94.
18. Prestwich R, Sykes J, Carey J, Sen M, Dyker K, et al. Improving target definition for head and neck radiotherapy: a place for magnetic resonance imaging and 18-fluoride fluorodeoxyglucose positron emission tomography? Clin Oncol. 2012;24:577-589.
19. Ashamalla H, Guirgius A, Bieniek E, Rafla S, Evola A, et al. The impact of positron emission tomography/computed tomography in edge delineation of gross tumor volume for head and neck cancers. Int J Radiat Oncol Biol Phys. 2007;68:388-395.
20. Grégoire V, Evans M, Le Q, Bourhis J, Budach V, et al. Delineation of the primary tumour clinical target volumes (ctv-p) in laryngeal, hypopharyngeal, oropharyngeal and oral cavity squamous cell carcinoma: Airo, caca, dahanca, eortc, georcc, gortec, hknpcsg, hncig, iag-kht, lprhht, ncic ctg, ncri, nrg oncology, phns, sbrt, somera, sro, sshno, trog consensus guidelines. Radiother Oncol. 2018;126:3-24.
21. Grégoire V, Ang K, Budach W, Grau C, Hamoir M, et al. Delineation of the neck node levels for head and neck tumors: a 2013 update. DAHANCA, EORTC, HKNPCSG, NCIC CTG, NCRI, RTOG, TROG consensus guidelines. Radiother Oncol. 2014;110: 172-181.
22. Brouwer C, Steenbakkers R, Bourhis J, Budach W, Grau C, et al. CT-based delineation of organs at risk in the head and neck region: DAHANCA, EORTC, GORTEC, HKNPCSG, NCIC CTG, NCRI, NRG Oncology and TROG consensus guidelines. Radiother Oncol. 2015;117:83-90.
23. Dubuisson M, Jain A. A modified Hausdorff distance for object matching. Proceedings of the International Conference on Pattern Recognition. Jerusalem. 1994;566-568.
24. Delouya G, Igidbashian L, Houle A, Belair M, Boucher L, et al. 18F-FDG-PET imaging in radiotherapy tumor volume delineation in treatment of head and neck cancer. Radiother Oncol. 2011;101:362-368.
25. Ahmed M, Schmidt M, Sohaib A, Kong C, Burke K, et al. The value of magnetic resonance imaging in target volume delineation of base of tongue tumours-a study using flexible surface coils. Radiother Oncol. 2010;94:161-167.
26. Samołyk-Kogaczewska N, Sierko E, Zuzda K, Gugnacki P, Jurgilewicz D et al. PET/MRI-guided GTV delineation during radiotherapy planning in patients with squamous cell carcinoma of the tongue. Strahlen Onkol. 2019;195:780-791.
27. Ferrando O, Scolarob T, Ciarmiello A, Foppiano F. Target volume definition and dosimetric issues in radiotherapy treatment of head and neck disease with FDG-PET/CT: A monocentric experience. J Diagn Imag Ther. 2018;5:14-19.
28. Kågedal Å, Rydberg Millrud C, Hayry V, Kumlien Georen S, Lidegran M, et al. Oropharyngeal squamous cell carcinoma induces an innate systemic inflammation, affected by the size of the tumour and the lymph node spread. Clin Otolaryngol. 2018; 43:1117-1121.
29. Daisne J, Duprez T, Weynand B, Lonneux M, Hamoir M, et al. Tumor volume in pharyngolaryngeal squamous cell carcinoma: comparison at CT, MR imaging, and FDG PET and validation with surgical specimen. Radiol. 2004;233:93-100.
30. Zrnc TA, Wallner J, Zemann W, Pau M, Gstettner C, et al. Assessment of tumor margins in head and neck cancer using a 3D-navigation system based on PET/CT image-fusion-a pilot study. J Craniomaxillofac Surg. 2018;46:617-623.
31. Beegam Sumayya AM, Krishnan AR. 2018. Ramifications of dental materials in head and neck MR imaging-a short review. Impressions - J IDA Attingal Branch. 2018;8:57-60.
32. Eggers G, Rieker M, Kress B, Fiebach J, Dickhaus H, et al. Artefacts in magnetic resonance imaging caused by dental material. Magn Reson Mater Phys Biol Med. 2005; 18:103-111.
33. Ladefoged C, Hansen A, Andersen F. Dental artifacts in the head and neck region: implications for Dixon-based attenuation correction in PET/MRI. Eur J Nucl Med Mol I Phys. 2005;2:8.
34. Kao CH, Hsieh TC, Yu CY, Yen KY, Yang SN, et al. 18 F-FDG PET/CT-based gross tumor volume definition for radiotherapy in head and neck cancer: a correlation study between suitable uptake value threshold and tumor parameters. Radiat Oncol. 2010; 5:76.
35. Paulino AC, Koshy M, Howell R, Schuster D, Davis LW. Comparison of CT-and FDG-PET-defined gross tumor volume in intensity-modulated radiotherapy for head-and-neck cancer. Int J Radiat Oncol Biol Phys. 2005;61:1385-1392.
36. Greco C, Nehmeh SA, Schoder H, Gonen M, Raphael B, et al. Evaluation of different methods of 18F-FDG-PET target volume delineation in the radiotherapy of head and neck cancer. Am J Clin Oncol. 2008;31:439-445.

37. Belli ML, Mori M, Broggi S, Cattaneo GM, Bettinardi V, et al. Quantifying the robustness of [18 F] FDG-PET/CT radiomic features with respect to tumor delineation in head and neck and pancreatic cancer patients. Phys Med. 2018;49:105-111.

38. Schinagl DAX, Vogel WV, Hoffmann AL, Van Dalen JA, Oyen WJ, et al. Comparison of five segmentation tools for 18f-fluoro-deoxy-glucose-positron emission tomography-based target volume definition in head and neck cancer. Int J Radiat Oncol Biol Phys. 2007;69:1282-1289.

39. Guardia MEB, Romasanta LP, Vincente AMG, Rubio MPT, Munoz AP, et al. Utility of PET-CT on radiotherapy planning of head and neck cancer. Our initial experience. Rev Esp Med Nucl (Eng Edition). 2010;29;157-164.

40. Wang K, Heron DH, Clump DA, Flickinger JC, Kubicek GJ, et al. Target delineation in stereotactic body radiation therapy for recurrent head and neck cancer: a retrospective analysis of the impact of margins and automated PET-CT segmentation. Radiother Oncol. 2013;106:90-95.

41. Mohamed ASR, Cardenas CE, Garden AS, Awan MJ, Rock CD, et al. Patterns-of-failure guided biological target volume definition for head and neck cancer patients: FDG-PET and dosimetric analysis of dose escalation candidate subregions. Radiother Oncol. 2017; 124:248-255.

42. Zegers CML, Van Elmpt W, Hoebers FJP, Troost EGC, Ollers MC, et al. Imaging of tumour hypoxia and metabolism in patients with head and neck squamous cell carcinoma. Acta Oncol. 2015;54:1378-1384.

43. Grégoire V, Eriksen J. Impact of hypoxia in head and neck cancer radiotherapy. Clin Transl Imaging. 2017;5:497-505.

44. Li Z, Lin X, Zang J, Wang X, Jin Z, et al. Kit formulation for preparation and biological evaluation of a novel 99mTc-oxo complex with metronidazole xanthate for imaging tumor hypoxia. Nucl Med Biol. 2016;43:165-170.

45. Zou KH, Warfield SK, Bharatha A, Tempany CM, Kaus MR, et al. Statistical validation of image segmentation quality based on a spatial overlap index. Acad Radiol. 2004;11:178-89.

46. Szyszko TA, Cook GJR. PET/CT and PET/MRI in head and neck malignancy. Clin Radiol. 2018;73:60-69.